Use of quantum correlation: A theoretical and experimental perspective

Prasanta K. Panigrahi[1,2] *AND Chiranjib Mitra*[1]

Abstract | Recent interest in the field of quantum information processing has given rise to a flurry of theoretical as well as experimental activity, on entanglement, a purely quantum mechanical phenomenon. We briefly review quantification of entanglement and its use in carrying out quantum tasks like teleportation. The measures are primarily concerned with bipartite entanglement. Systems such as spin chains and quantum dots have been identified to execute some of these quantum protocols. Experimental realization of quantum networks, especially in the form of spin chains, has been dealt here, along with methods to extract the content of entanglement from experimental data. We explicate the effect of environment on quantum networks and how to extract quantum information before the system decoheres.

1. Introduction

Correlations, peculiar to the quantum world, have led to prolonged debates about the nature of many particle quantum systems. The fact, two systems together can, in some precise sense, represent more than the independent subsystems, is at the root of this debate. Schrödinger[1], realized the physical importance of non-separability of multi-particle quantum systems and coined the word, "entanglement". Einstein, Podolsky and Rosen (EPR) then utilized this property of wave-functions to highlight the possibility of "spooky action at a distance", in the quantum world[2]. Quantitative understanding of quantum correlation arose from Bell's work[3], which led to a precise difference between quantum mechanics and deterministic hidden variable theories. It is, hence, quite satisfying that this correlation, in recent times, has led to many profound developments in quantum computation and information theory[4,5]. Entanglement has played a significant role in many practical applications, like quantum teleportation, dense coding, information splitting, quantum key distribution and quantum games, to name a few.

In the realization of these protocols, finite dimensional Hilbert spaces have played a significant role. The measure of entanglement, for multipartite systems in finite dimensional Hilbert spaces, is still an area of active research. For continuous variable systems, apart from the two particle Gaussian states, not much is known. It is interesting to note that in the area of quantum information theory, the well studied physical systems, like harmonic oscillator and hydrogen atom, are yet to make a significant impact.

In the subsequent sections, we briefly review certain topics, where our own research interests lie. First we give a brief exposition of entanglement and its measure in section 2. Then we introduce teleportation through entangled channels, where we also include teleportation in non-maximally entangled states. In section 3, we discuss the

[1]*Indian Institute of Science Education and Research (IISER) Kolkata, Mohanpur Campus, P.O. BCKV Campus Main Office, Mohanpur - 741252, Nadia, West Bengal, India*
[2]*Physical Research Laboratory, Navrangpura, Ahmedabad 380009, India*
pprasanta@iiserkol.ac.in
chiranjib@iiserkol.ac.in

experimental realization of entangled channels and how to induce an entangling gate in spin chains, by controlling the sign of the exchange interaction in a low spin, low dimensional system. We also support our results with density functional theory calculations, which match with the experimental results to a great extent. In the following section (4), we deal with entanglement witnesses in spin chains and how to extract the entanglement content from experimental data. Here we illustrate magnetic susceptibility as an ideal entanglement witness in the case of spin chains and fit experimental data to demonstrate this claim. We then cover teleportation in the presence of environmental effects, leading to decoherence, in section 5. An interesting feature here is bath induced entanglement. In the following section (6), we analyze state characterization of three particle states and their utility in teleportation. This is followed in section 7, by physical realization of a three particle entangled state, from a product state, by switching on Heisenberg interaction. Here, we also extend our methodology to a N-qubit channel. It is followed by a brief conclusion and future directions in the final section.

2. Role of entanglement in teleportation

Physical realization of entangled bipartite systems are quite common. The fact that fermions and bosons possess symmetric and antisymmetric wavefunctions, respectively, naturally leads to entangled states. For example, a two particle fermionic system, where, the space part is symmetric under exchange of particles, has the spin part in the singlet form: $|\psi\rangle_{\text{singlet}} = \frac{1}{\sqrt{2}}[|\uparrow\rangle_1|\downarrow\rangle_2 - |\downarrow\rangle_1|\uparrow\rangle_2]$, where $|\uparrow\rangle = |0\rangle = \begin{pmatrix} 1 \\ 0 \end{pmatrix}$ and $|\downarrow\rangle = |1\rangle = \begin{pmatrix} 0 \\ 1 \end{pmatrix}$ are the two orthogonal states, known as qubits. This is a member of the well known Bell states:

$$|\psi_\pm\rangle = \frac{1}{\sqrt{2}}[|\uparrow\rangle_1|\downarrow\rangle_2 \pm |\downarrow\rangle_1|\uparrow\rangle_2], \quad (1)$$

$$|\phi_\pm\rangle = \frac{1}{\sqrt{2}}[|\uparrow\rangle_1|\uparrow\rangle_2 \pm |\downarrow\rangle_1|\downarrow\rangle_2], \quad (2)$$

which has been extensively used in quantum computation. Before proceeding further, it is instructive to study the nature of entanglement, in these so called maximally entangled states. For this purpose, the density matrix approach is well suited, where the density matrix, $\rho = |\psi\rangle\langle\psi|$, for a pure state. Working it out explicitly for one of the cases, e.g., the singlet state, $|\psi_-\rangle = \frac{1}{\sqrt{2}}[|\uparrow\rangle_1|\downarrow\rangle_2 - |\downarrow\rangle_1|\uparrow\rangle_2]$, we obtain,

$$\rho = |\psi_-\rangle\langle\psi_-| = \rho_{12} = \frac{1}{2}\begin{pmatrix} 0 & 0 & 0 & 0 \\ 0 & 1 & -1 & 0 \\ 0 & -1 & 1 & 0 \\ 0 & 0 & 0 & 0 \end{pmatrix} \quad (3)$$

To quantify entanglement, one computes the reduced density matrix of this state by tracing out one of the particles, say particle 2, which leads to,

$$\rho_1^{\text{red}} = \frac{1}{2}\begin{pmatrix} 1 & 0 \\ 0 & 1 \end{pmatrix}. \quad (4)$$

where ρ_1^{red} represents a maximally mixed state, containing two diagonal elements of equal value. For a mixed state, $Tr(\rho_{red}^2) < 1$. For pure states, the reduced density matrix will have only one diagonal element.

Given a density matrix, ρ, the von-Neumann entropy, which is a measure of entanglement, is given as, S(ρ) = -Tr(ρ ln(ρ). It can be expressed in terms of the eigen values of ρ: $S(\rho) = -\Sigma_i \lambda_i \log(\lambda_i)$, where the logarithm is taken with base 2. For pure states, as expected, $S(\rho)$ is zero. In the above case for ρ_1^{red}, representing a mixed state,

$$S(\rho_1^{\text{red}}) = -\text{Tr}(\rho_1^{\text{red}} \cdot \ln(\rho_1^{\text{red}})) = \log(2) = 1. \quad (5)$$

Thus for this maximally entangled bipartite state, the entanglement measure is "1"; the two particles share "1" e-bit of entanglement. It is worth noting that, if the system is a product state like $|0\rangle|1\rangle$, then tracing out one particle will not affect the other particle of the state, leading to a pure reduced density matrix. The purity of a density matrix is checked by the idempotent nature of the matrix; since as mentioned earlier, a pure state has only one diagonal element.

In a seminal paper, Bennett *et al.*[6], demonstrated teleportation of a single qubit state, using the Bell state as an entangled channel. In their protocol, there are two parties, Alice and Bob, sharing the entangled state and Alice has the state, $|\psi_1\rangle = \alpha|0_1\rangle + \beta|1_1\rangle$ ($|\alpha|^2 + |\beta|^2 = 1$), which needs to be teleported. Alice wishes to transfer this quantum state to Bob without directly sending the particle to him. Any quantum measurement performed by Alice on $|\psi_1\rangle$ will destroy the quantum state at hand, without revealing all the necessary information to Bob for reconstructing the quantum state. However, this problem can be circumvented by using an ancillary pair of entangled particles 2 and 3 (an EPR pair), where particle 2 is given to Alice and particle 3 to Bob, such that, $|\psi_-\rangle = \frac{1}{\sqrt{2}}[|0\rangle_2|1\rangle_3 - |1\rangle_2|0\rangle_3]$. The important property of this entangled state is that, as soon as a measurement on one of the particles is performed projecting it onto a certain state, which can be any normalized linear superposition of $|0\rangle$ and $|1\rangle$, the other particle has to be in the orthogonal state. Although, the particles 1 and 2 are not entangled, their combined state can always be expressed as a superposition of the four

maximally entangled Bell states, since these states form a complete orthonormal basis in 4 dimensional Hilbert space. The full state of the 3 particles can be written as:

$$|\psi_{123}\rangle = \frac{1}{\sqrt{2}}[|\psi_{12}^-\rangle(-\alpha|0_3\rangle - \beta|1_3\rangle) + |\psi_{12}^+\rangle (-\alpha|0_3\rangle + \beta|1_3\rangle) + |\phi_{12}^-\rangle(\alpha|1_3\rangle + \beta|0_3\rangle) + |\phi_{12}^+\rangle(\alpha|1_3\rangle - \beta|0_3\rangle)]. \quad (6)$$

Alice now performs a Bell measurement on particles 1 and 2, i.e., she projects her two particles onto one of the 4 Bell states. As a result, Bob's particle will be in a state that is directly related to the initial state, $|\psi_1\rangle$. For example, if the result of Alice's measurement is $|\psi_{12}^+\rangle$, then particle 3, which is with Bob, has to be in the state $(-\alpha|0_3\rangle + \beta|1_3\rangle)$. Hence, all that Alice has to do after her measurement, is to inform Bob via a classical channel the final state of her measurement and Bob can perform an appropriate local unitary transformation ($U = \begin{pmatrix} -1 & 0 \\ 0 & 1 \end{pmatrix}$ for the above case), on his particle 3 in order to obtain the initial state of particle 1, since, $U(-\alpha|0\rangle_3 + \beta|1\rangle_3) = \alpha|0\rangle_3 + \beta|1\rangle_3$.

Note that, during the teleportation process, the values of α and β remain unknown. By her measurement, Alice does not obtain any information, whatsoever, about the teleported state. All that is achieved by a Bell measurement is a transfer of the quantum state. Thus in Bennett *et al*.'s protocol, Alice first combines the unknown qubit with her state and performs a Bell measurement and communicates the result of her measurement to Bob via two cbits of information corresponding to four Bell states. Bob, then performs an appropriate local unitary operation and obtains the unknown qubit.

The importance of maximally entangled states can be appreciated from the following teleportation protocol. One starts with a minimal deformation for the maximally entangled state[7], which form a mutually orthogonal basis,

$$|\phi_l^+\rangle = \frac{1}{\sqrt{1+|\ell|^2}}(|00\rangle + l\,|11\rangle), |\phi_l^-\rangle = \frac{1}{\sqrt{1+|\ell|^2}}(l^*|00\rangle - |11\rangle), \quad (7)$$

and

$$|\psi_p^+\rangle = \frac{1}{\sqrt{1+|p|^2}}(|01\rangle + p\,|10\rangle), |\psi_p^-\rangle = \frac{1}{\sqrt{1+|p|^2}}(p^*|01\rangle - |10\rangle). \quad (8)$$

Here l and p are complex numbers in general. When $l = p = 0$, this basis reduces to the computational basis $[\{|00\rangle, |01\rangle, |10\rangle, |11\rangle\}]$, which is not entangled. For $l = p = 1$, it reduces to the maximally entangled Bell basis. One can verify that the von-Neumann entropies of the above non-maximally entangled states are not the same, unlike the Bell states, where they are all same (1 ebit of entanglement).

Following the teleportation protocol, one has to combine Alice's qubit ($|\psi_1\rangle = \alpha|0_1\rangle + \beta|1_1\rangle$) with the resource state,

$$|\phi\rangle_{23} = \frac{1}{\sqrt{1+|n|^2}}(|00\rangle_{23} + n|11\rangle_{23}), \quad (9)$$

which is a non-maximally entangled state. The combined state can be written as,

$$\begin{aligned}|\psi\rangle_1|\phi\rangle_{23} &= N\,(\alpha|0\rangle_1 + \beta|1\rangle_1)\,(|00\rangle_{23} + n|11\rangle_{23}) \\ &= N\,(\alpha|00\rangle_{12}|0\rangle_3 + \alpha\, n|01\rangle_{12}|1\rangle_3 + \beta|10\rangle_{12}|0\rangle_3 \\ &+ \beta\, n|11\rangle_{12}|1\rangle_3) \\ &= N[\,|\phi_l^+\rangle_{12}\,(L\,\alpha|0\rangle_3 + L\,n\,\beta\,l^*|1\rangle_3) \\ &+ |\phi_l^-\rangle_{12}(L\,l\,\alpha|0\rangle_3 - n\,L\,\beta|1\rangle_3) \\ &+ |\psi_p^+\rangle_{12}(P\,\beta\,p^*|0\rangle_3 + P\,\alpha\,n|1\rangle_3) + |\psi_p^-\rangle_{12} \\ &(-P\,\beta|0\rangle_3 + P\,\alpha\,n\,p|1\rangle_3)]. \end{aligned} \quad (10)$$

Here $N = \frac{1}{\sqrt{1+|n|^2}}$, $L = \frac{1}{\sqrt{1+|\ell|^2}}$ and $P = \frac{1}{\sqrt{1+|p|^2}}$ are real numbers. Above expression is the most general way of rewriting an unknown state and two qubit non-maximally entangled state. Agrawal and Pati[7] considered the case $l = n = p^*$, for which, the basis used for joint measurements (Eq. 7–8) and the resource state (Eq. 9) have the same amount of quantum entanglement (von-Neumann entropy), $S(|\phi\rangle) = (-N^2\log_2 N^2 - N^2\,|n|^2\log_2 N^2|n|^2)$. Supposing, the outcome is $|\phi_{l=n}^-\rangle$, then the state at Bob's end will be $(\alpha|0\rangle - \beta|1\rangle)$ and when the outcome is $|\psi_{p=n}^+\rangle$, then the state at Bob's end is $(\beta|0\rangle + \alpha|1\rangle)$. Therefore, after Alice communicates with Bob, he will apply σ_z in the former and σ_x in the later case to recover the unknown state with unit fidelity. For the other two states, the teleportation protocol fails. The net probability of successful teleportation, considering both the events would be,

$$P_{\text{succ}} = \frac{2|n|^2}{(1+|n|^2)^2}. \quad (11)$$

Thus, using $S(|\phi\rangle) = (-N^2\log_2 N^2 - N^2\,|n|^2\log_2 N^2|n|^2)$ amount of entanglement and

one c-bit Alice can teleport an unknown state with a probability given in Eq. 11. This probability goes from zero for seperable ($l = n = p = 0$) to one-half for the maximally entangled resource state. The other half comes from the other two maximally entangled states, or from the other two events, i.e., when the outcome of Alice's measurement is either $|\phi^+\rangle$ or $|\psi^-\rangle$.

Thus we see that teleportation is deterministic only for a maximally entangled channel, whereas it is probabilistic for non-maximally entangled channels. We will return to this feature in a later section, when we deal with decoherence in an entangled channel and how it affects teleportation. In physical systems, there will always be some interaction with the environment, which will lead to gradual reduction in entanglement. However, in some cases, the interaction of two qubits with a common bath can lead to bath induced entanglement, which results in an enhancement in entanglement. We will see the consequence of teleportation in such a channel in section 5.

3. Experimental realization – spin chains

In this section, we briefly describe magnetic systems with exchange interaction and show their relevance to quantum computation, in particular, the possible sign change of the exchange interaction with structure in thin films[8,9]. The importance of such a feature is that, if one can induce antiferromagnetism in a ferromagnetic system, then it is akin to a control NOT (CNOT) gate, provided it is a quantum mechanical system. It is necessary that the system be a low dimensional, low spin system. Magnetic systems, where this feature can be explored, are spin chains of low spin value (spin 1/2 or spin 3/2). It is also imperative to have materials that can be integrated with existing technology, i.e., semiconductor devices. Many magnetic semiconductors are quite promising in this regard. However, the design and fabrication of materials that exhibit both semiconducting and magnetic properties for spintronics[10] and quantum computing has proven difficult. Important starting points are high-purity thin films, as well as fundamental theoretical understanding of magnetism in these systems. Here, we show that small molecules have great potential in this area because of the ease of insertion of localized spins in organic frameworks and also because of both chemical and structural purity. In particular, we demonstrate that archetypal molecular semiconductors, namely the metal phthalocyanines, can be readily fabricated as thin film quantum antiferromagnets and represent an important precursor to a solid state quantum computer. These materials behave like a spin chain, since they have a strong anisotropic magnetic exchange; z-component of the exchange is an order of magnitude higher than the x and y components. Their magnetic state can be switched via fabrication steps that modify the film structure, offering practical routes to information processing. Theoretical calculations show that a new mechanism, which is the molecular analogue of the interactions between magnetic ions in metals, is responsible for the observed magnetic states. This combination of theory and experiments opens the field of organic thin film magnetic engineering.

Phthalocyanines (abbreviated Pc for the phthalocyanato ion $C_{32}H_{16}N_8^{2-}$) are polyaromatic molecules which can accommodate a range of atoms or groups of atoms (in the 2+ oxidation state) in their central cavity[11]. They have now become archetypal organic semiconductors, and their attractive optoelectronic properties are already being extensively exploited in solar cells[12], field effect transistors, and light emitting diodes[13]. Magnetic studies have been comparatively sparse, and have mainly focused on MnPc single crystals, which exhibit ferromagnetism below about 10 K[14]. The influence of crystal structure on magnetic properties has recently become apparent via pressure-dependent investigations[15], dopant-induced crystal modification[16], and film studies[17].

One of the experimental challenges leading up to a workable quantum computer, is fabrication of quantum gates, which needs useful spin entanglement. Entanglement in ordered solids is most easily achieved for low dimensional, low spin ions, with antiferromagnetic coupling. These conditions are fulfilled by CuPc, where molecules form chain-like stacks and are each in the $S = 1/2$ state due to the Cu^{2+} ion. We have therefore, chosen to fabricate and characterize CuPc thin films, and have extended our studies to CuPc crystals to estimate the influence of structure and spin state on magnetic coupling[8].

Organic molecular beam deposition (OMBD) in an ultrahigh-vacuum (UHV) chamber enables the formation of Pc thin films with a high degree of control and versatility. Various flexible films, optimized for magnetic measurements, were grown on thermally stable polyimide substrates (Kapton) by this method. The thickness of all films studied is typically 60 nm, and the morphology of a CuPc film deposited on Kapton at room temperature, shows that it forms small spherical crystallites. This is characteristic of planar phthalocyanines evaporated onto an amorphous substrate and is usually attributed to the so-called α-phase[17]. The polymorphic phase is confirmed by powder X-ray diffraction. The molecules are arranged in a

Table 1: Magnetic correlations of different materials

–	β-CuPc crystal	β-CuPc film	α-CuPc film
θ_p(K)	−0.40	0.0	−2.6
J_{exBF}(K)	0.15	0.0	−1.4
J_{exDFT}(K)	−0.25	−0.25	−1.75

herringbone fashion, with their molecular planes parallel to each other within a column and forming an angle $\phi = 65°$ with respect to the stacking direction. The films are highly textured with the (b, c) plane parallel to the substrate. Post-growth annealing of the α-CuPc film at 320 °C, leads to a phase transition to the β-polymorph, which is characterized by elongated crystallites, and a more compact structure, with ϕ reduced to 45°. The intra-stack intermolecular separation is 3.4 Å, the lateral shift between successive molecules in the β-phase is 3.4 Å, which is, more than twice the value of 1.6 Å for the α-phase. Single crystals of CuPc, which belong to the β-phase, were obtained by gradient sublimation.

Fig. 1 exhibits the main magnetic measurements on CuPc films and single crystals. Both the Curie-Weiss plots and magnetization curves show clearly the switching of the magnetism between α and β polymorphs for Pc containing either transition metal. For the thin film α phase, the Curie-Weiss plot has negative intercept θ_p and the crossover to full saturated magnetization, in the M-H curve, corresponds to large fields. This implies strong antiferromagnetic correlations that are only destroyed at elevated temperatures or high fields. On the other hand, for both the thin film and bulk crystalline β-phases, we see that in the case of Cu, θ_p is close to zero, and the magnetization curves are close to those for a Brillouin function for free $S = 1/2$ ions having Landé-g factor, $g = 2$. It can therefore be concluded that the magnetic couplings are mainly determined by the intermolecular shifts within columns, irrespective of physical appearance, crystal orientation, or inter-column interactions. These small shifts (< 2 Å) are able to modify the magnetic characteristics of the material, and the $\alpha \rightarrow \beta$ phase transition corresponds to a conversion of the material from antiferro to paramagnetic. The antiferromagnetic $S = 1/2$ chains along the stacks are quantum antiferromagnets with strongly entangled spins, implying more significantly, that a very straightforward annealing procedure switches the interactions of these interesting quantum objects. This is akin to a C-NOT or entangling gate.

Table 1 shows the results of the Curie-Weiss analysis of the magnetization for the different films, and clearly illustrates the polymorphic switching effects that are possible in the new nanocrystalline system of transition metal Pc films. For low dimensional magnets, the observed values for θ_p are proportional to, but actually somewhat larger than, the exchange coupling; this follows because the Curie-Weiss form does not reproduce the well-known cusp in the susceptibility of the $S = 1/2$ Heisenberg antiferromagnetic chain. To extract values of the coupling constant, J_{exBF}, appearing in the chain Hamiltonian $H = \Sigma_i J_{exBF} \vec{S_i}.\vec{S_{i+1}}$, we neglect interchain interactions, as well as the effects of potential dimerizations. We performed a global fit to the Bonner-Fisher model[19] for all field-dependent and temperature-dependent magnetizations in the range of 0–7 Tesla and 2–30 K. Values of J_{exBF} for the different CuPc samples obtained by this fit are listed in Table 1. The switching behavior seen in the Curie-Weiss constants is reproduced, and the antiferromagnetic exchange constants J_{exBF} are smaller than θ_p, as expected.

Thus, it can be seen that one can engineer magnetic couplings using polymorphism in transition metal Pc films. To understand the couplings in the different CuPc polymorphs, ab initio calculations were performed to determine the values of the exchange interactions from total energy differences. The details of the calculations can be found in Ref. 18. Absolute values were computed as a function of ϕ by comparing the energies of the singlet (estimated using the broken-symmetry approach developed by Noodelman[20]) and triplet states in a CuPc dimer, as calculated by density functional theory (DFT) with the Gaussian code[21] and the B3LYP or UB3LYP exchange-correlation functionals[22,23], which give good descriptions of exchange interactions in organic systems[24]. For ϕ values of 45° and 65°, astonishingly good agreement between experiment and theory is observed, that is, the antiferromagnetic interaction is favored in both cases, with $J = 1.75$ K in the α phase, while the coupling is comparably negligible in the β phase ($J = 0.25$ K). One interesting finding from the calculations is the possibility of sign changes, that is, switching between antiferro- and ferromagnetism, in the exchange interactions as a function of ϕ, which occur between 30° and 40°.

Though the theoretical results match remarkably well with experiment, it is important to develop some intuition as to the origin of this effect, and in particular the possibility of a sign change in J as a function of ϕ. This is a very important result, since this will enable us to change the sign of the exchange from ferromagnetic to anti-ferromagnetic by tuning the structure. Since these films could be grown on Kapton, which is a very flexible material, it is in principle possible to tune the structure by bending the films. A sign change of the exchange

Figure 1: Magnetic properties of phthalocyanine films and crystals. (a) Temperature-dependent susceptibility of a range of CuPc films and crystals, with corresponding linear fits to the Curie-Weiss law (dashed line) and Bonner-Fisher fits (solid line). (b) Field dependent magnetisation for the CuPc films and crystals taken at 2 K with resulting fits to the Bonner-Fisher model.

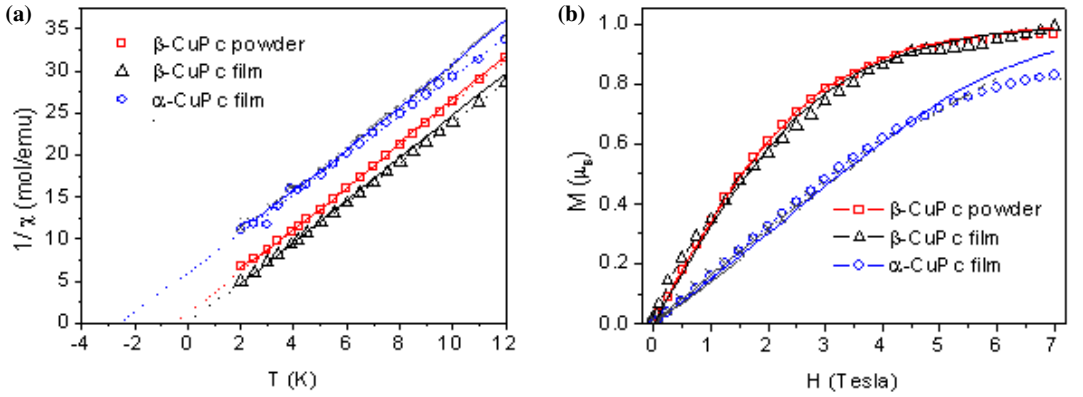

constant is nothing but a control NOT (C-NOT) gate, in a low dimensional, low spin system. The conventional mechanism for magnetic coupling between localized transition-metals involves super-exchange[25], where an electron hops on and off the transition metal via the highest occupied or lowest unoccupied molecular orbitals (HOMO or LUMO, respectively). In CuPc, there are no MOs with the same symmetry as the Cu_{II} ion (b_{1g}) near the Fermi edge, thus ruling out super-exchange. Instead, we have proposed that the magnetic coupling occurs via indirect exchange[25], where the Pc system is transiently polarized by the direct Coulomb interaction with the Cu_{II} spin, and this polarization is then transferred to the neighboring molecule by the hopping of a polarized electron-hole pair. This mechanism requires the electron and hole to occupy orbitals of the same symmetry, and the two e_g levels just below and above the Fermi level satisfy this criterion. Perturbation theory to second order in the pair creation amplitude, and second order in the hopping matrix elements (t_e and t_h for electron and hole, respectively, evaluated using the Kohn-Sham states obtained from DFT) leads to an exchange coupling which is directly proportional to $t_e t_h$. The interactions are weakly ferromagnetic at small ϕ, and negligible at $\phi = 45°$, consistent with the experimentally observed behaviour in β-CuPc. For increasing ϕ, the coupling then becomes anti-ferromagnetic, as observed in the negative J values obtained in α CuPc. A qualitative understanding of the trends in $t_e t_h$ can be obtained from looking at the contributions to the overlap integrals for the orbitals involved, namely e_g (HOMO) and e_g (LUMO). The mechanism implied in the perturbation theory is the molecular analogue of the Ruderman-Kittel-Kasuya-Yosida (RKKY)[26] interaction between localized moments in metals, and gives a qualitative explanation of the form of J, including the possibility of sign changes, but does not fully reproduce all features of the DFT calculations.

Therefore, polymorphic phthalocyanine films represent a new system where a molecular semiconductor is endowed with magnetic properties that can be switched with slight changes in crystal structure. In addition to illustrating this process based on a simple annealing procedure, one can in principle come up with routes for reversible switching using, for instance, mechanical stress. Although the transition temperatures are still low, our theoretical estimates show that these can be improved with further crystal modifications, and DFT will assist us to choose optimized materials and structures. Further enhancement in operation temperatures can be expected from using doping or more complex material systems combined with our controlled growth methods. Using local annealing, templating, and isomorphous substitution of different phthalocyanine derivatives, it will be possible to create new types of multilayer heterostructures which will provide a highly versatile ground for the development of new devices for quantum computation, without the requirements of epitaxy and compatibility, which can restrict inorganic materials.

4. Entanglement in spin chains

In the previous section we have investigated materials which are manifested in the form of

spin chains and where quantum gate operations like CNOT can be performed. Here we investigate the entanglement properties of states obtained through temporal evolution of specific seed states. Experimental detection of entanglement in spins systems requires a suitable entanglement witness as well as a means to extract entanglement quantitatively from experimental data. There has been significant progress in this area[29–32] and we explore magnetic susceptibility as a possible entanglement witness in this section. This is followed by extraction of entanglement from experimental data. The Hamiltonian of a spin chain with nearest neighbour interaction, is given by,

$$\mathcal{H} = J\sum_i \vec{S}_i \cdot \vec{S}_{i+1} + B\sum_i S_i^z \qquad (12)$$

where, the spins are given by (in the unit of $\hbar$=1), $S_i = \frac{\sigma_i}{2}; i = 1,2,3$ and $\sigma_1 = \begin{pmatrix} 0 & 1 \\ 1 & 0 \end{pmatrix}; \sigma_2 = \begin{pmatrix} 0 & -i \\ i & 0 \end{pmatrix}; \sigma_3 = \begin{pmatrix} 1 & 0 \\ 0 & -1 \end{pmatrix}$ are the three Pauli spin matrices.

If the external magnetic field is assumed to be applied along the $\hat{z}$ direction, the net magnetization would be defined as the expectation value of σ_3, the eigenvectors of which are $|\uparrow\rangle = \begin{pmatrix} 1 \\ 0 \end{pmatrix}$ and $|\downarrow\rangle = \begin{pmatrix} 0 \\ 1 \end{pmatrix}$.

Since most of the measures of entanglement currently available are for bipartite systems, it would be interesting to see if we can extract the bipartite entanglement from a given magnetization data for a spin chain. In this section we will concentrate mostly on qubits, i.e., on spin half systems. The Hamiltonian for two qubit system can be written as:

$$\begin{aligned} \mathcal{H} &= J\vec{S_1}\cdot\vec{S_2} + B(S_1^z + S_2^z) \\ &= \frac{J}{4}(\sigma_1^x\cdot\sigma_2^x + \sigma_1^y\cdot\sigma_2^y + \sigma_1^z\cdot\sigma_2^z) \\ &\quad + \frac{B}{2}(\sigma_1^z + \sigma_2^z) \end{aligned} \qquad (13)$$

$$\begin{aligned} &= \frac{J}{4}\begin{pmatrix} 1 & 0 & 0 & 0 \\ 0 & -1 & 2 & 0 \\ 0 & 2 & -1 & 0 \\ 0 & 0 & 0 & 1 \end{pmatrix} + \frac{B}{2}\begin{pmatrix} 2 & 0 & 0 & 0 \\ 0 & 0 & 0 & 0 \\ 0 & 0 & 0 & 0 \\ 0 & 0 & 0 & 2 \end{pmatrix} \\ &= \begin{pmatrix} \frac{J}{4}+B & 0 & 0 & 0 \\ 0 & -\frac{J}{4} & \frac{J}{2} & 0 \\ 0 & \frac{J}{2} & -\frac{J}{4} & 0 \\ 0 & 0 & 0 & \frac{J}{4}-B \end{pmatrix}. \end{aligned} \qquad (14)$$

The eigenvalues and the corresponding eigenvectors of this Hamiltonian are: $E_1 = \frac{J}{4} + B$; $|\uparrow\uparrow\rangle = \begin{pmatrix} 1 \\ 0 \\ 0 \\ 0 \end{pmatrix}$, $E_2 = \frac{J}{4} - B$; $|\downarrow\downarrow\rangle = \begin{pmatrix} 0 \\ 0 \\ 0 \\ 1 \end{pmatrix}$, $E_3 = \frac{J}{4}$;

$|\psi^+\rangle = \frac{1}{\sqrt{2}}(|\uparrow\downarrow\rangle + |\downarrow\uparrow\rangle) = \frac{1}{\sqrt{2}}\begin{pmatrix} 0 \\ 1 \\ 1 \\ 0 \end{pmatrix}$, $E_4 = -\frac{3J}{4}$;

$|\psi^-\rangle = \frac{1}{\sqrt{2}}(|\uparrow\downarrow\rangle - |\downarrow\uparrow\rangle) = \frac{1}{\sqrt{2}}\begin{pmatrix} 0 \\ 1 \\ -1 \\ 0 \end{pmatrix}$, where

$|\psi^+\rangle$ and $|\psi^-\rangle$ are the Bell states.

In the ground state (at low temperatures) the system is in the lowest eigenvalue state $|\psi^-\rangle$, which is a pure state. As we have seen in section I, this is a maximally entangled state as the reduced density matrix is maximally mixed. However, at finite temperatures the system is in a mixed state,

$$\begin{aligned} \rho &= \frac{1}{Z}\{|\phi^-\rangle\langle\phi^-|e^{\frac{3J}{4}\beta} + |\phi^+\rangle\langle\phi^+|e^{-\frac{J}{4}\beta} + |\uparrow\uparrow\rangle \\ &\langle\uparrow\uparrow|e^{-(\frac{J}{4}-B)\beta} + |\downarrow\downarrow\rangle\langle\downarrow\downarrow|e^{-(\frac{J}{4}+B)\beta}\} \\ &= \frac{1}{Z}\begin{pmatrix} e^{-(\frac{J}{4}-B)\beta} & 0 & 0 & 0 \\ 0 & e^{-\frac{J}{4}\beta}+e^{\frac{3J}{4}\beta} & e^{-\frac{J}{4}\beta}-e^{\frac{3J}{4}\beta} & 0 \\ 0 & e^{-\frac{J}{4}\beta}-e^{\frac{3J}{4}\beta} & e^{-\frac{J}{4}\beta}+e^{\frac{3J}{4}\beta} & 0 \\ 0 & 0 & 0 & e^{-(\frac{J}{4}+B)\beta} \end{pmatrix}, \end{aligned} \qquad (15)$$

where $\beta = \frac{1}{k_B T}$ and $Z = Tr(\rho) = e^{\frac{3J}{4}\beta} + e^{\frac{-J}{4}\beta} + e^{(\frac{-J}{4}+B)\beta} + e^{(\frac{-J}{4}-B)\beta}$.

Now let us consider the high temperature limit ($\beta \to 0$), the density matrix reduces to,

$$\begin{aligned} \rho &= \frac{1}{4}\begin{pmatrix} 1&0&0&0 \\ 0&1&0&0 \\ 0&0&1&0 \\ 0&0&0&1 \end{pmatrix} = \frac{1}{4}\begin{pmatrix} 1&0&0&0 \\ 0&0&0&0 \\ 0&0&0&0 \\ 0&0&0&0 \end{pmatrix} \\ &\quad + \frac{1}{4}\begin{pmatrix} 0&0&0&0 \\ 0&1&0&0 \\ 0&0&0&0 \\ 0&0&0&0 \end{pmatrix} + \frac{1}{4}\begin{pmatrix} 0&0&0&0 \\ 0&0&0&0 \\ 0&0&1&0 \\ 0&0&0&0 \end{pmatrix} \\ &\quad + \frac{1}{4}\begin{pmatrix} 0&0&0&0 \\ 0&0&0&0 \\ 0&0&0&0 \\ 0&0&0&1 \end{pmatrix} \end{aligned} \qquad (16)$$

A mixed state ρ is separable if it can be expressed as a convex sum of tensor product states of the two

subsystems. In this case, there exists $p_k \geq 0$, such that $\rho = \sum_k p_k \rho_1^k \otimes \rho_2^k$, for $\sum_k p_k = 1$, where $\{\rho_1^k\}$ and $\{\rho_2^k\}$, are pure ensembles of the appropriate subsystems. Otherwise ρ is called an entangled state[33]. ρ in Eq. (16) can be expressed as,

$$\rho = \frac{1}{4}\begin{pmatrix}1&0\\0&0\end{pmatrix}\otimes\begin{pmatrix}1&0\\0&0\end{pmatrix}+\frac{1}{4}\begin{pmatrix}0&0\\0&1\end{pmatrix}\otimes\begin{pmatrix}1&0\\0&0\end{pmatrix} +\frac{1}{4}\begin{pmatrix}1&0\\0&0\end{pmatrix}\otimes\begin{pmatrix}0&0\\0&1\end{pmatrix}+\frac{1}{4}\begin{pmatrix}0&0\\0&1\end{pmatrix}\otimes\begin{pmatrix}0&0\\0&1\end{pmatrix}. \tag{17}$$

Hence the system is perfectly separable and the first term of the Hamiltonian (Eq. 13) becomes,

$$\begin{aligned}\langle\vec{\sigma}_1\cdot\vec{\sigma}_2\rangle &= \langle\sigma_x^1\sigma_x^2\rangle+\langle\sigma_y^1\sigma_y^2\rangle+\langle\sigma_z^1\sigma_z^2\rangle \\ &= \langle\sigma_x^1\rangle\langle\sigma_x^2\rangle+\langle\sigma_y^1\rangle\langle\sigma_y^2\rangle+\langle\sigma_z^1\rangle\langle\sigma_z^2\rangle\end{aligned} \tag{18}$$

Since the Pauli spin matrices are traceless, $\langle\sigma_x^1\rangle\langle\sigma_x^2\rangle+\langle\sigma_y^1\rangle\langle\sigma_y^2\rangle+\langle\sigma_z^1\rangle\langle\sigma_z^2\rangle = 0$. This can be easily verified using $\langle\sigma_x^1\rangle = \mathrm{Tr}(\rho\sigma_x^1)$, etc., and using the separable ρ given in Eq. 16.

To calculate the thermal entanglement (i.e., for intermediate temperatures), one writes the density matrix for an N-particle state, in the most general form,

$$\rho = \sum_i p_i \rho_i^1 \otimes \rho_i^2 \otimes \cdots \otimes \rho_i^N \tag{19}$$

The free energy, U, by definition, is the expectation value of the Hamiltonian, i.e., $U = \langle\mathcal{H}\rangle$ and the magnetization, M, is defined as the sum of the expectation values of the $\hat{z}$-component of individual spins, $M = \sum_{i=1}^N \langle\sigma_z^i\rangle$. Therefore, from Eq. 12, one can obtain,

$$\frac{U-BM}{NJ} = \frac{1}{4N}\left|\sum_{i=1}^{N}(\langle\sigma_x^i\sigma_x^{i+1}\rangle+\langle\sigma_y^i\sigma_y^{i+1}\rangle +\langle\sigma_z^i\sigma_z^{i+1}\rangle)\right|, \tag{20}$$

since, $\vec{S} = \frac{1}{2}\vec{\sigma}$. If the density matrix is separable, i.e., if they can be expressed as a convex sum, such that, $\sum_i p_i = 1$, $\forall p_k \geq 0$, then the R.H.S of Eq. 20 becomes separable, and for every i one has,

$$\begin{aligned}&|\langle\sigma_i^x\sigma_{i+1}^x\rangle+\langle\sigma_i^y\sigma_{i+1}^y\rangle+\langle\sigma_i^z\sigma_{i+1}^z\rangle| = |\langle\sigma_i^x\rangle\langle\sigma_{i+1}^x\rangle \\ &+\langle\sigma_i^y\rangle\langle\sigma_{i+1}^y\rangle+\langle\sigma_i^z\rangle\langle\sigma_{i+1}^z\rangle| \\ &\leq\sqrt{\langle\sigma_i^x\rangle^2+\langle\sigma_i^y\rangle^2+\langle\sigma_i^z\rangle^2} \\ &\sqrt{\langle\sigma_{i+1}^x\rangle^2+\langle\sigma_{i+1}^y\rangle^2+\langle\sigma_{i+1}^z\rangle^2}\leq 1.\end{aligned} \tag{21}$$

The upper bound was found by using the Cauchy-Schwarz inequality and the fact that for any state $\langle\sigma^x\rangle^2+\langle\sigma^y\rangle^2+\langle\sigma^z\rangle^2 \leq 1$. If this inequality is violated, the system is in an entangled state. Thus the condition for entanglement is $\frac{|U-BM|}{N|J|} > 1$, which in absence of magnetic field, reduces to, $\frac{|U|}{N|J|} > 1$.

In a ferromagnetic ground state, in absence of magnetic field, $\langle\vec{\sigma_i}\cdot\vec{\sigma_{i+1}}\rangle$ will always be zero and hence it is not an entangled state. This is because the order parameter (magnetization) commutes with the Hamiltonian and there is no spin fluctuation at lower temperatures. This can be easily shown in a two qubit system, since the $\vec{\sigma_i}\cdot\vec{\sigma_{i+1}}$ term of the Hamiltonian can be rewritten as $\sigma_i{}^+\cdot\sigma_{i+1}{}^- + \sigma_i{}^-\cdot\sigma_{i+1}{}^+ + 2\sigma_3$, where $\sigma^\pm = \sigma_1 \pm i\sigma_2$. One can see by inspection that $\langle\sigma_i{}^+\cdot\sigma_{i+1}{}^-\rangle = \langle\uparrow\uparrow|\,\sigma_i{}^+\cdot\sigma_{i+1}{}^-\,|\uparrow\uparrow\rangle = 0$. Thus the order parameter $\langle\sigma_3\rangle$ commutes with the Hamiltonian. The effect of temperature and magnetic field on the entanglement of a Heisenberg ferromagnet has been dealt by Arnesen, Bose and Vedral[34], wherein they consider the effect of magnons on entanglement.

It has been shown by Wootters[35], that concurrence is a good measure of entanglement, which is given by,

$$\mathcal{C} = \max(\sqrt{\lambda_1}-\sqrt{\lambda_2}-\sqrt{\lambda_3}-\sqrt{\lambda_4}), \tag{22}$$

where $\lambda_1 \geq \lambda_2 \geq \lambda_3 \geq \lambda_4$, are the eigenvalues of the operator,

$$\tilde{\rho}_{12} = \sigma_2\otimes\sigma_2\rho_{12}^*\sigma_2\otimes\sigma_2, \tag{23}$$

such that, ρ_{12} is the two particle reduced density matrix and the asterisk denotes complex conjugation. It has been shown by O'Connor, and Wootters[36], that for an antiferromagnet, the concurrence is given by,

$$\mathcal{C} = \frac{1}{2}\ \mathrm{max}\left[0, \frac{|U|}{NJ}-1\right], \tag{24}$$

in absence of magnetic field. Now, for a bipartite system, $\langle\vec{\sigma}_1\cdot\vec{\sigma}_2\rangle = \langle\sigma_x^1\sigma_x^2\rangle+\langle\sigma_y^1\sigma_y^2\rangle+\langle\sigma_z^1\sigma_z^2\rangle$. Considering the system to be isotropic, we obtain, $\langle\sigma_x^1\sigma_x^2\rangle = \langle\sigma_y^1\sigma_y^2\rangle = \langle\sigma_z^1\sigma_z^2\rangle$. Condition 21 can be rewritten as, $|\langle\vec{S}_1\cdot\vec{S}_2\rangle| = |\langle S_x^1S_x^2\rangle+\langle S_y^1S_y^2\rangle+\langle S_z^1S_z^2\rangle| = |\langle S_x^1\rangle\langle S_x^2\rangle+\langle S_y^1\rangle\langle S_y^2\rangle+\langle S_z^1\rangle\langle S_z^2\rangle| \leq |\vec{S}_1||\vec{S}_2| \leq 1/4$. Thus, the formula for concurrence, given in Eq. 24, can be written as,

$$\mathcal{C} = 2\ \mathrm{max}\left[0, \langle\vec{S}^1\cdot\vec{S}^2\rangle-(1/4)\right]. \tag{25}$$

One can evaluate, from the bipartite Hamiltonian (Eq. 13), for the B=0 limit, $\langle \vec{S}^1 \cdot \vec{S}^2 \rangle = (\frac{3}{4}) \frac{1-e^{-\frac{J}{kT}}}{1+3e^{-\frac{J}{kT}}}$[37]. Thus we have,

$$\mathcal{C} = 2\max\left[0, \frac{1-3e^{-\frac{J}{kT}}}{1+3e^{-\frac{J}{kT}}}\right] \tag{26}$$

Recently, magnetic susceptibility has been shown to be a macroscopic entanglement witness[29]. To extract the entanglement from experimental data, one has to express concurrence in terms of a measurable quantity, e.g., magnetic susceptibility. The magnetic susceptibility, χ, can be defined as the field derivative of magnetization (in the applied field direction, which here is $\hat{z}$) in the limit $B \to 0$. Thus,

$$\chi = \left(\frac{\delta M}{\delta B}\right) = (g^2\mu_B^2/kT)\langle M^2\rangle_{B=0} = (g^2\mu_B^2/kT) \sum_{i,j}\langle {S_i}^z S^z_{i+1}\rangle \approx (g^2\mu_B^2 N/kT)[(1/4) + (\langle \vec{S}_1 \cdot \vec{S}_2\rangle)/3]. \tag{27}$$

Here we have used the isotropy of space, nearest neighbour interaction, and the identity $\vec{S}_1 \cdot \vec{S}_2 = \frac{1}{2}[(\vec{S}_1 + \vec{S}_2)^2 - \vec{S}_1^2 - \vec{S}_2^2]$ and the fact that $(\vec{S}_1 + \vec{S}_2)$=0 for an antiferromagnet. From Eq's (25) and (27) one can obtain the concurrence in terms of susceptibility,

$$\mathcal{C} = \max\left[0, 1 - \frac{(6k_B T\chi)}{g^2\mu_B^2 N}\right]. \tag{28}$$

Since one has $|\langle \vec{S}_1 \cdot \vec{S}_2\rangle| \leq 1/4$ for any separable state (Eq. (21)), the magnetic susceptibility for such states will satisfy,

$$\chi \geq \frac{g^2\mu_B^2 N}{kT}\frac{1}{6}. \tag{29}$$

Now we consider an archetypal spin chain, a compound copper nitrate, having spin half and exhibiting antiferromagnetic interactions, with a Néel temperature, T_N= 5K[38]. A digitized data was obtained from Ref. 38, and was fitted to the formulae for susceptibility given in Eq. 27 (see Fig. 2(a)). The dotted line shows the entanglement boundary given by Eq. 29; the entangled region is represented by the region towards the left of the dotted line. It is evident that the copper spins exhibit entanglement below the antiferromagnetic ordering temperature. Fig. 2(b), shows the extracted value of concurrence and the fit to Eq. 26, for $J = 5$ K. Thus entanglement witness is, not only an entity which is quantifiable, but it also is something that can be measured experimentally.

We have also extended the above analysis to the results of CuPC films forming in the α-phase as studied in the last section. The two point correlation function calculated for neighbouring spins, was fitted to the magnetization data. Here we assumed a singlet-triplet (or dimer) model, so that nature favours the antiferromagnetic interaction (only nearest neighbour). We consider the full Hamiltonian where the magnetic field "H" is also included to fit the experimental magnetization vs. field data. In Fig. 3, the variation of energy with magnetic field is depicted diagrammatically. In absence of the field, there will be threefold degenerate triplet states with energy "$\frac{J}{4}$" and a singlet state with energy "$\frac{-3J}{4}$". However in presence of magnetic field, the energy levels corresponding to the Bell states $|\phi_\pm\rangle$ (Eq. 1), fan out as shown in the Fig. 3(b), their energy eigenvalues given by "$\frac{J}{4} \pm B$" respectively.

In absence of magnetic field, the antiferromagnetic interaction forces the system to be in singlet state (at low temperatures) and with increase in magnetic field, the system makes a gradual transition to the triplet state (see Fig. 3(c)). If the magnetic field is applied in the $\hat{z}$-direction, the relevant order parameter would be the expectation value of the total spin in $\hat{z}$-direction, and the magnetization M, is given by $M = \langle S_z^{\text{Total}}\rangle = \langle S_z^1 + S_z^2\rangle$.

The partition function for this dimer is given by, $\mathcal{Z} = \text{Tr}[\rho_0]$, where ρ_0=exp[$-\frac{\mathcal{H}}{k_B T}$] and the Hamiltonian $\mathcal{H}$ is given by Eq. 13.

The magnetization M, in the dimer model, is then given by,

$$M = \text{Tr}(\rho \cdot S_z^{\text{Total}}) = \frac{2\sinh(2g\mu_B H k_B T)}{1 + 2\cosh(2g\mu_B H k_B T) + \exp(J/k_B T)}, \tag{30}$$

where "g" is the Landé g factor. We have fitted the CuPC magnetization data taken at $T = 2$ K, to Eq. 30 and it is shown in Fig. 4. We have taken the value of $J = 2$ K, consistent with the x-axis intercept in the χ^{-1} vs T curve (Fig. 1(a)). We have also plotted the simulated curves for Brillouin spin $\frac{1}{2}$ (unpaired spins) and Brillouin spin 1 (triplet case) to compare with the data. In the triplet case (spin 1), we have scaled the values for spin pairing (two sites of spin half each giving rise to a spin 1 site). The value of magnetization in our data is less than the Brillouin spin $\frac{1}{2}$ value at low

Figure 2: (a) Fitting of susceptibility data (solid line) to Eq. 27. The dotted line marks out the separable regime (Eq. 29) from the entangled regime (see text) (b) Extraction of concurrence from the susceptibility data of copper nitrate using Eq. 28.

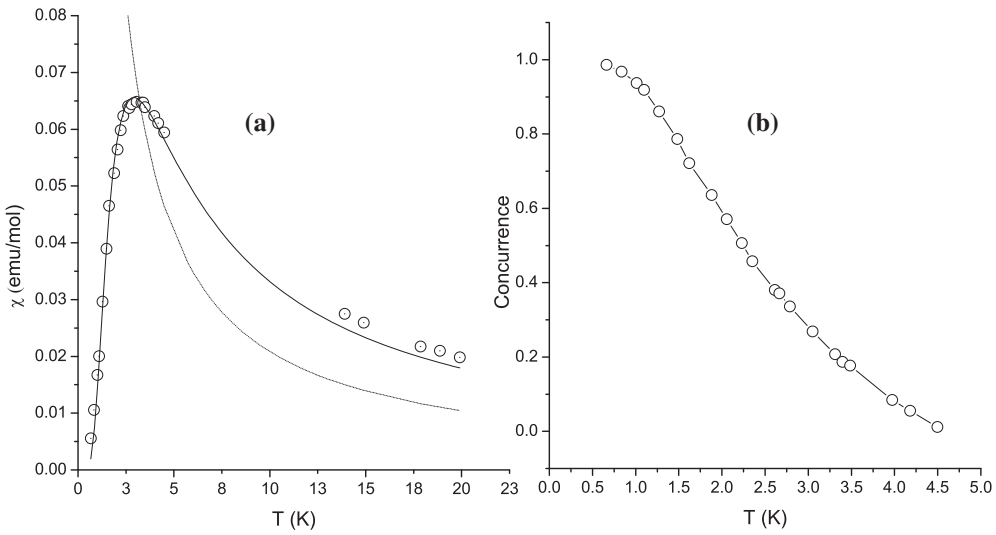

Figure 3: Dimer model for simulating the result of magnetization data of CuPc (a). Energy level diagram as a function of field for singlet and triplet states (b). The spin $\frac{1}{2}$ pairs can either combine as singlet (spin 0) or triplet (spin 1) (c).

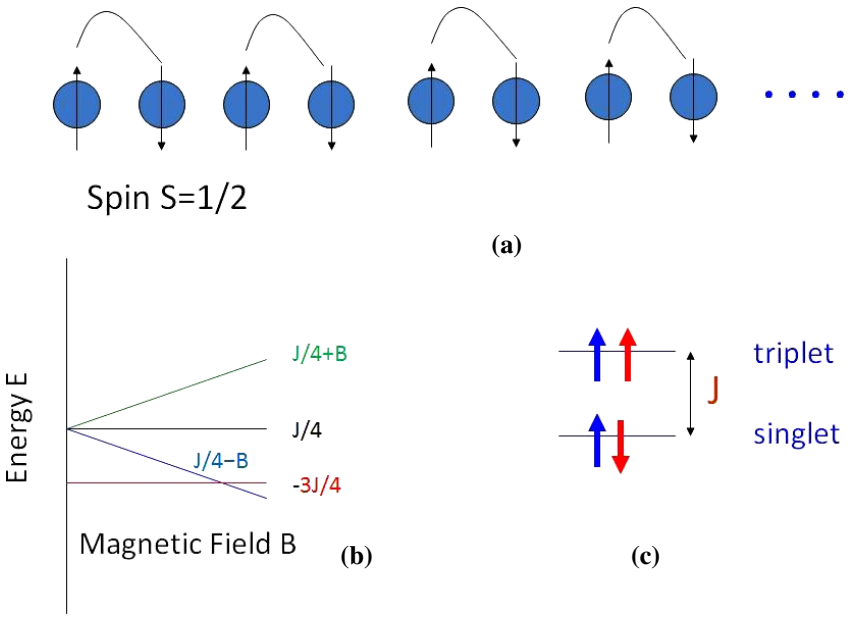

fields (≤ 6 Tesla), which signifies the presence of antiferromagnetic interaction, and is indicative of entanglement expected in low spin, low dimensional systems. To fit the temperature dependence, we need to go down to lower temperatures, since the θ_P in this case is about 1.8 K (see last section). The magnetization for Brillouin spin 1 (pure triplet case) is given by,

$$M = \frac{2\sinh(2g\mu_B H k_B T)}{1+2\cosh(2g\mu_B H k_B T)}, \qquad (31)$$

Figure 4: Magnetization data of CuPc fitted to the singlet-triplet model (thick red line). The spin $\frac{1}{2}$ Brillouin function and the triplet (spin 1) magnetization is also shown. The data and the fit to singlet-triplet model show that the interactions are antiferromagnetic, since it is below the Brillouin spin $\frac{1}{2}$ value at low field, merging with the data only at high fields. The Brillouin spin 1 curve has been halved, since the number of spins forming the triplet is twice that of the total unpaired spin $\frac{1}{2}$ electrons.

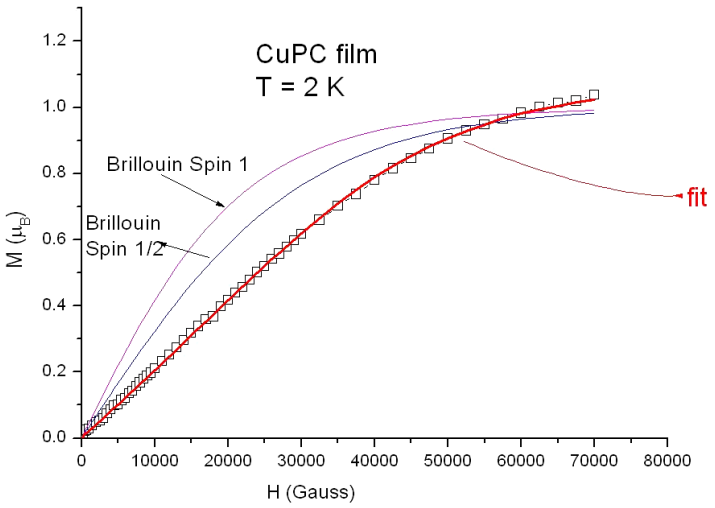

and that of spin $\frac{1}{2}$ is given by,

$$M = \tanh(g\mu_B H k_B T), \tag{32}$$

Eq. 31 can be obtained by setting $J \to -\infty$, i.e., in the presence of a strong ferromagnetic coupling, where all the spins are rendered parallel and hence in the triplet state. On the other hand, Eq. 32 can be obtained by setting $J \to 0$, where there is no coupling and all the spins behave like free spins and get aligned with increasing magnetic field at a fixed temperature. Both these limits ($J \to -\infty$ and $J \to 0$) are classical limits and hence represent separable states.

5. Decoherence of two particle

Quantum protocols are mostly designed in the idealistic situation of a decoherence free system. In practical implementation of these protocols the external environment can play a significant role in reducing the fidelity of the expected outcomes. In implementing quantum teleportation[44], Bob gets the desired unknown state after a proper unitary transformation, irrespective of the Bell state measurement made by Alice. The same may not be true in presence of environmental interaction, which can be present both at the transmitting and the receiving stations. The decoherence at the transmitting station can be quite different from that of the receiving station, since Alice is in possession of two qubits, where as Bob has only one. If the qubits of Alice see different environments, there is nothing new to the dynamics as Bob gets the same decohered state irrespective of the Bell state shared with Alice. On the other hand if both the qubits of Alice see a common environment, there will be bath mediated interaction between the two. This can lead to the bath induced entanglement between Alice's qubits[39]. The common environment for Alice's qubits is a more natural choice to study the effects of decoherence on teleportation and we briefly review the same below.

Writing the qubit states in terms of the polarizations and correlations helps one understand the underlying physical structure in a straightforward manner. The density matrix for a qubit is represented by,

$$\rho(\vec{P}) = \frac{1}{2}(\hat{\mathcal{I}} + \vec{P}.\vec{\sigma}), \tag{33}$$

where $\vec{P} = Tr(\rho\vec{\sigma})$ and $\vec{\sigma} = \hat{i}\sigma_x + \hat{j}\sigma_y + \hat{k}\sigma_z$.

The most general representation of a two-qubit Bell state is given by

$$\rho_{AB} = \frac{1}{4}\hat{\mathcal{I}} + \sum_k D_k S_A^k S_B^k, \tag{34}$$

where S_A^k and S_B^k are the spin operators of the qubits A and B respectively, with the correlation vector $D_k \equiv \mathrm{Tr}(\rho_{AB} S_A^k S_B^k)$. For the Bell states the corresponding correlation vectors are

given by $\vec{D}_{S_0} = [-1,-1,-1]$, $\vec{D}_{T_0} = [1,1,-1]$, $\vec{D}_{T_+} = [1,-1,1]$, and $\vec{D}_{T_-} = [-1,1,1]$. The Bell states are represented as $|S_0\rangle = \frac{1}{\sqrt{2}}[|\uparrow\downarrow - \downarrow\uparrow\rangle]$, $|T_0\rangle = \frac{1}{\sqrt{2}}[|\uparrow\downarrow + \downarrow\uparrow\rangle]$, $|T_+\rangle = \frac{1}{\sqrt{2}}[|\uparrow\uparrow + \downarrow\downarrow\rangle]$ and $|T_-\rangle = \frac{1}{\sqrt{2}}[|\uparrow\uparrow - \downarrow\downarrow\rangle]$. $|S_0\rangle$ is the singlet and the other three belong to the triplet sector. When evolving through Hamiltonian dynamics each of them respond differently to the environmental interaction and to the applied fields. Note that we have used new notations for Bell states here for convenience, as opposed to the notations used in section 2.

Using the Bell-state representation given above, the initial state, used in the teleportation protocol, is given by

$$\begin{aligned}\rho_{aAB} &= \rho_a \otimes \rho_{AB} \\ &= \frac{1}{2}\left[\hat{\mathcal{I}} + 2\vec{P}_a \cdot \vec{S}_a\right] \\ &\quad \otimes \frac{1}{4}\left[\hat{\mathcal{I}} + 4\sum_k D_k S_A^k S_B^k\right], \end{aligned} \tag{35}$$

where $\vec{P}_a = \mathrm{Tr}\rho_a \vec{S}_a$ is the polarization vector of the unknown state which is to be teleported to Bob. Now Alice performs a Bell state measurement on her two qubits a and A, i.e.,

$$\mathrm{Tr}_{aA}[\rho_{aA} \otimes \hat{\mathcal{I}}_B \rho_{aAB}], \tag{36}$$

where $\rho_{aA} = \frac{1}{4}\hat{\mathcal{I}} + \sum_k M_k S_a^k S_A^k$ is the Bell state of qubits a, A. The vector $\vec{M}$ has the information of the Bell measurement made by Alice. After performing the trace, the state that Bob gets with $1/4$ probability is given by

$$\rho_B = \frac{1}{2}\left[\hat{\mathcal{I}} + 2\vec{P}_B \cdot \vec{S}_B\right]. \tag{37}$$

The polarization of Bob's qubit is related to the polarization of the unknown state through the correlation vectors D and M as

$$P_B^i = D_i M_i P_a^i. \tag{38}$$

Now if the vectors $\vec{D}$ and $\vec{M}$ are equal, Bob needs to do nothing to this qubit. If $(\vec{D} \times \vec{M}) \cdot \hat{n} \neq 0$, then Bob has to do a rotation of his qubit along $\hat{n}$ direction. Performing the appropriate unitary transformation is equivalent to multiplying $D_i M_i$ to P_B^i in Eq. 38. Since $D_i^2 = M_i^2 = 1$, we see that the final state of Bob is the unknown state that Alice wishes to teleport. The above representation helps in dealing with the time-evolution of the qubits in the presence of environment. The Hamiltonian describing the interaction between the qubits and the spin bath is given by

$$H = K_a \vec{S}_a \cdot \vec{I}_{\mathcal{E}a} + K_A \vec{S}_A \cdot \vec{I}_{\mathcal{E}A} + K_B \vec{S}_B \cdot \vec{I}_{\mathcal{E}B}, \tag{39}$$

where $\vec{S}_a, \vec{S}_A$, represents the spin operators of the two qubits at the transmitting site which are in possession of Alice and $\vec{S}_B$ is the spin operator of Bob's qubit. The total spin of the environmental particles seen by each qubit is represented by $\vec{I}_{\mathcal{E}} = \sum_k \vec{I}_{\mathcal{E},k}$. The interaction strengths of the qubits with their respective baths are denoted by K_a, K_A and K_B. Since decoherence at Bob's site is trivial, we set $K_B = 0$ and study the effects of a common bath decoherence of Alice's qubits on fidelity of the teleported state. The Hamiltonian given in Eq. 39 reduces to

$$H = (K_a \vec{S}_a + K_A \vec{S}_A) \cdot \vec{I}_{\mathcal{E}}, \tag{40}$$

where $\vec{I}_{\mathcal{E}}$ represents the total bath spin. Note that eventhough there is no direct interaction between Alice's qubits, their interaction with the bath can result in an indirect coupling between the two.

We shall take the initial state of the bath as an incoherent superposition of states labelled by the bath spin $I_{\mathcal{E}}$, with weights $\lambda_{I_{\mathcal{E}}}$, $\rho_{\mathcal{E}}(0) = \sum \lambda_{I_{\mathcal{E}}} \rho_{I_{\mathcal{E}}}(0)$. In this study all $\rho_{I_{\mathcal{E}}}(0)$ will be taken to be unpolarized (multiple of identity), with weights $\lambda_{I_{\mathcal{E}}}$ as free parameters.

We rewrite the initial state of the Alice-Bob system given in Eq.35 as,

$$\begin{aligned}\rho_{aAB}(0) &= \frac{1}{8}\hat{\mathcal{I}} + \frac{1}{2}\vec{P}_a \cdot \vec{S}_a + \frac{1}{2}\vec{\mathbb{P}}_A \cdot \vec{S}_A \\ &\quad + \sum_{m,n=1}^{3} \mathbb{D}_{mn} S_a^m S_A^n, \end{aligned} \tag{41}$$

by absorbing Bob's spin $\vec{S}_B$ into the polarization vectors. The components of the new polarization vectors are $\mathbb{P}_A^i = D_i S_B^i$, and $\mathbb{D}^{mn} = P_a^m D^n S_B^n$. Since the time-evolution is only for qubits a and A, the above form is valid.

The state of the total system before Alice makes the Bell measurement is time-dependent, given by

$$\rho_{aAB}(t) = \mathrm{Tr}_{\mathcal{E}}\left(U_H(t)\rho_{aAB}(0) \otimes \rho_{\mathcal{E}} U_H^{\gamma}(t)\right), \tag{42}$$

where $\mathrm{Tr}_{\mathcal{E}}$ represents the summing over the bath degrees of freedom. Note that the initial state of the system-bath is uncorrelated. In the above equation

the unitary operator U_H, corresponding to the Hamiltonian in Eq. 40, is given by

$$\begin{aligned} U_H &= \Big[a_1(t)+a_2(t)(\vec{S}_a-\vec{S}_A)\cdot\vec{I}_{\mathcal{E}}\Big] \\ &\times\left(1-\frac{\hat{S}^2_{aA}}{2}\right)+\Big[a_3(t)+a_4(t)\vec{S}_{aA}\cdot\vec{I}_{\mathcal{E}} \\ &+a_5(t)(\vec{S}_{aA}\cdot\vec{I}_{\mathcal{E}})^2 a_6(t)(\vec{S}_a-\vec{S}_A)\cdot\vec{I}_{\mathcal{E}} \\ &+a_7(t)(\vec{S}_a\times\vec{S}_A)\cdot\vec{I}_{\mathcal{E}}\Big]\frac{\hat{S}^2_{aA}}{2}, \end{aligned} \tag{43}$$

where $\vec{S}_{aA}=\vec{S}_a+\vec{S}_A$. After performing the trace over bath degrees of freedom, we obtain the reduced density matrix of the Alice-Bob system,

$$\begin{aligned} \rho_{aAB}(t) &= \frac{1}{8}\hat{\mathcal{I}}+\frac{1}{2}\vec{P}_a(t)\cdot\vec{S}_a+\frac{1}{2}\vec{\mathbb{P}}_A(t)\cdot\vec{S}_A \\ &+\sum_{m,n=1}^{3}\mathbb{D}_{mn}(t)S^m_a S^n_A. \end{aligned}$$

After Alice makes the Bell measurement on her qubits, the state that Bob gets with 1/4 probability is given by

$$\rho_B(t)=\frac{1}{2}\hat{\mathcal{I}}+\sum_k M_k\mathbb{D}_{kk}(t), \tag{44}$$

with $\mathbb{D}_{kk}(t)$ given by

$$\begin{aligned} \mathbb{D}_{kk}(t) &= f(t)\mathbb{D}_{kk}(0)+g(t)\mathrm{Tr}[\mathbb{D}(t)], \\ &= f(t)P^k_a D_k S^k_B+g(t)\sum_m P^m_a D_m S^m_B \end{aligned} \tag{45}$$

Depending on the two bits of classical information given by Alice, Bob makes the appropriate unitary transformation. The final state of Bob is then given by

$$\rho_B(t)=\frac{1}{2}\hat{\mathcal{I}}+\vec{P}_B(t)\cdot\vec{S}_B, \tag{46}$$

where $P^i_B=f(t)P^i_a+g(t)M_i\mathrm{Tr}MP^i_a$. As expected, if system bath interaction is zero i.e., $K_a=K_A=0$ then $f(t)=1$, $g(t)=0$, and we get perfect teleportation. In the presence of the bath Bob's final state depends on $\vec{M}$ from which he can know about the measurement made by Alice. Note that there is no information of M in decoherence free teleportation after Bob has made his final transformation. One can show that if the qubits of Alice see separate environments there will be no such dependence of Alice measurement. Hence common bath has introduced a new feature to the protocol, where Bob's final state has the information of the Bell measurement made by Alice.

Let us calculate the fidelity and average fidelity of teleportation in the presence of decoherence. Fidelity gives the information of how close is the teleported state to the unknown state, defined as

$$\begin{aligned} \mathcal{F}(t) &\equiv \frac{1}{2}\big[1+\vec{P}_a\cdot\vec{P}_B(t)\big], \\ &= \frac{1}{2}\left[1+f(t)|\vec{P}_a|^2+g(t)\mathrm{Tr}M\sum_k(P^k_a)^2M_k\right]. \end{aligned} \tag{47}$$

By performing an average over all pure states of qubit a we get the average fidelity,

$$\begin{aligned} \mathcal{F}_{av}(t) &= \frac{1}{4\pi}\int_0^{2\pi}d\phi\int_0^{\pi}d\theta\sin\theta\mathcal{F}(t), \\ &= \frac{1}{2}\left[1+f(t)+\frac{1}{3}g(t)(\mathrm{Tr}M)^2\right]. \end{aligned} \tag{48}$$

We restrict to the leading order time-dependence of the time-dependent coefficients $f(t)$ and $g(t)$ in studying the short time behavior, and for long time behavior we give the appropriate numerical plots.

The leading order time dependence of the coefficients $f(t)$ and $g(t)$ are

$$\begin{aligned} f(t) &\approx 1-\frac{1}{3}\{\langle\hat{I}^2_{\mathcal{E}}\rangle(K^2_a+K^2_A+K_aK_A)\}t^2, \\ g(t) &\approx \frac{1}{3}\langle\hat{I}^2_{\mathcal{E}}\rangle K_aK_At^2. \end{aligned} \tag{49}$$

If $K_a=K_A$ then $f(t)+3g(t)=1$. Now substituting these time-dependent coefficients in Eq. 48, we find

$$\begin{aligned} \mathcal{F}_{av}(t) &= 1-\frac{t^2}{12}\langle\hat{I}^2_{\mathcal{E}}\rangle(K^2_a+K^2_A)\,[1 \\ &+\Delta(1-(\mathrm{Tr}M)^2/3\big] \end{aligned} \tag{50}$$

where the inhomogeneity parameter $\Delta=2K_AK_a/(K^2_A+K^2_a)$ and $\langle\hat{I}^2_{\mathcal{E}}\rangle=\sum_{I_{\mathcal{E}}}\lambda_{I_{\mathcal{E}}}I_{\mathcal{E}}(I_{\mathcal{E}}+1)$. For completely unpolarized baths i.e., $\rho_{\mathcal{E}}=\frac{1}{2^N}\hat{\mathcal{I}}$, $\langle\hat{I}^2_{\mathcal{E}}\rangle=3N/4$, where N is number of bath spins.

For Bell states TrM has only two values, $-3, 1$. If the state is singlet, then $\mathrm{Tr}M=-3$ and for the remaining Bell states it has the value one. The average fidelity has an initial Gaussian decay, $\mathcal{F}_{av}(t)=\exp(-t^2/\tau^2)$, with two different

decoherence time scales depending on the Bell state measurement made by Alice, given by

$$\left(\frac{1}{\tau^2}\right)_{S_0} = \frac{1}{6}\langle \hat{I}_{\mathcal{E}}^2\rangle (K_a^2 + K_A^2)(1-\Delta),$$
$$\left(\frac{1}{\tau^2}\right)_{T_0,T_+,T_-} = \frac{1}{6}\langle \hat{I}_{\mathcal{E}}^2\rangle (K_a^2 + K_A^2)\left(1+\frac{\Delta}{3}\right). \quad (51)$$

The Bell states S_0, T_0, T_+, T_- are the ones mentioned before in this section. When the couplings are identical i.e., $K_a = K_A$, $\Delta = 1$, the singlet measurement on Alice's qubits does not harm the state teleported to Bob. On the other hand if the sign of Δ becomes negative i.e., if one of Alice's qubit is interacting ferromagnetically with the bath and the other antiferromagnetically, then singlet measurement would give a highly decohered state to Bob in comparison to the other Bell measurements. Hence, the sign of the interaction with the bath can decide which particular measurement of Alice can give Bob a less decohered state.

Thus in teleporting an unknown state to Bob when Alice's qubits see a common environment, the average fidelity varies with the Bell state measurement performed by Alice. Even after Bob's operation, the state still has the information of Alice's measurement. This feature cannot be seen both in the decoherence free teleportation and teleportation through local noisy channels (separate baths). The singlet measurement always gives Bob the unknown state with high fidelity, only when both the qubits of Alice interact either ferromagnetically or antiferromagnetically with bath. In contrast, if one of the Alice's qubits interact ferromagnetically and the other antiferromagnetically then measurement of Bell states belonging to the triplet sector will give better fidelity.

6. State characterization and teleportation using three particle states

Teleportation of an unknown state has been demonstrated using entangled photons[67], atomic states[68], spin states in Nuclear Magnetic Resonance[69] and other solid state systems[70]. The usage of multi-particle entangled states for implementing a similar protocol was studied initially, using three and four qubit GHZ states[71]. In addition to the N-qubit GHZ states, W states form another class of entangled states, and are well studied for their high symmetry. W states can be generated from any N-qubit interactions which conserve the $\hat{z}$ component of the total spin of qubits.

The symmetric three qubit W state, $|\psi\rangle = \frac{1}{\sqrt{3}}[|100\rangle + |010\rangle + |001\rangle]$ fails to teleport the unknown state to Bob. In this connection, Agrawal and Pati[7] have proposed a modification of the W state which can teleport the unknown state perfectly. We will consider this modified W state along with the W state in this section.

As noted earlier, one of the most essential properties of a state to be used for quantum tasks like teleportation, dense coding and QIS, is entanglement. For multi-particle systems, two particle entanglement has been successfully formulated and various measures have been given, for pure as well as mixed states. To calculate the two particle entanglement in a multi-particle system, one can construct a density matrix and trace out the rest of the particles and then find the entanglement of the two remaining particles (qubits) by checking the purity (or the lack of it) of the reduced density matrix. This holds for pure states only and the entanglement can be quantified by calculating the von-Neumann entropy[4]. For mixed states, Peres-Horodecki criteria is a good measure for entanglement[72] and so is concurrence. Concurrence has an advantage, in the sense that, it gives a comparison for relative entanglement between qubits in a multi-particle system, where the monogamy inequality can be formulated as follows:

$$\sum_{i=2}^{n} C_{A_1A_i}^2 \leq C_{A_1|A_2\ldots A_n}^2. \quad (52)$$

Here $C_{A|B}$ represents the concurrence between subsystems A and B.

We now examine the entanglement in a few states with certain tasks like teleportation in mind. Let us first consider the W state given by:

$$|W\rangle = \frac{1}{\sqrt{3}}(|100\rangle + |010\rangle + |001\rangle), \quad (53)$$

and name particle 1 as A, particle 2 as B and particle 3 as C. Now tracing over particle 3 (or C), we obtain the reduced density matrix,

$$\rho_{AB} = \frac{1}{3}\begin{pmatrix} 1 & 0 & 0 & 0 \\ 0 & 1 & 1 & 0 \\ 0 & 1 & 1 & 0 \\ 0 & 0 & 0 & 0 \end{pmatrix}. \quad (54)$$

This reduced density matrix has only two non-zero eigenvalues, $\lambda_1 = 2/3, \lambda_2 = 1/3$. Similarly,

$$\rho_{AC} = \frac{1}{3}\begin{pmatrix} 1 & 0 & 0 & 0 \\ 0 & 1 & 1 & 0 \\ 0 & 1 & 1 & 0 \\ 0 & 0 & 0 & 0 \end{pmatrix}. \quad (55)$$

One finds that, $\rho_{AB} = \rho_{AC} = \rho_{BC}$. The concurrence $C_{AB} = \frac{\sqrt{2}}{3} = C_{AC}$.

Tracing over the second (in ρ_{AB}) or third particle (in ρ_{AC}), we obtain,

$$\rho_A = \frac{1}{3}\begin{pmatrix} 2 & 0 \\ 0 & 1 \end{pmatrix}. \tag{56}$$

Here also there is a symmetry, $\rho_A = \rho_B = \rho_C$, hence, $C_{A(BC)} = \frac{2\sqrt{2}}{3}$. Thus,

$$C_{AB}^2 + C_{AC}^2 = C_{A|(BC)}^2. \tag{57}$$

Since the reduced density matrix $\rho_{AB} = \rho_{AC}$ has only two non-zero eigenvalues, each pair of qubits is entangled with only one other qubit, in a joint pure state. The formula for concurrence inequality simplifies in this case and it makes sense to speak of concurrence $C_{A(BC)}$ between qubit A and the pair BC. This is because, even though the state space of "BC" is four-dimensional, only two of those dimensions are necessary to express the pure state of ABC in their standard basis (i.e., $|0\rangle, |1\rangle$ basis). The equality in this case suggests that the entanglement between A and BC is shared equally between B and C. In general however, the amount of entanglement between A and BC cannot be accounted for by the entanglements of A with B and C separately. The difference between the two is the residual entanglement. Thus in a pure three particle state $|W\rangle$, the residual entanglement is zero.

Let us now consider the modified $|W\rangle$ state where there is an asymmetry of the form:

$$|W'\rangle = \frac{1}{2}(|100\rangle + |010\rangle + \sqrt{2}|001\rangle) \tag{58}$$

Following the above prescription, one finds,

$$\rho_{AB} = \frac{1}{4}\begin{pmatrix} 2 & 0 & 0 & 0 \\ 0 & 1 & 1 & 0 \\ 0 & 1 & 1 & 0 \\ 0 & 0 & 0 & 0 \end{pmatrix}. \tag{59}$$

This reduced density matrix has only two non-zero eigenvalues, $\lambda_1 = 2/3, \lambda_2 = 1/3$. Similarly,

$$\rho_{AC} = \frac{1}{4}\begin{pmatrix} 1 & 0 & 0 & 0 \\ 0 & 1 & \sqrt{2} & 0 \\ 0 & \sqrt{2} & 2 & 0 \\ 0 & 0 & 0 & 0 \end{pmatrix}. \tag{60}$$

In this case there is a slight asymmetry with respect to ρ_{AB} and ρ_{AC}, though both of them have only two non-zero eigenvalues – $\lambda_1 = 2/3, \lambda_2 = 1/3$ for ρ_{AB} and $\lambda_1 = 2/3, \lambda_2 = 1/3$ for ρ_{AC}. Using the same argument as in the $|W\rangle$ state, we obtain the concurrence $C_{A|BC} = \frac{\sqrt{3}}{2}$. The concurrence $C_{AB} = \frac{1}{2}$ and $C_{AC} = \frac{1}{\sqrt{2}}$. Thus, here too we get:

$$C_{AB}^2 + C_{AC}^2 = C_{A|(BC)}^2. \tag{61}$$

Measure of entanglement and its distribution over the qubits, in the sense how much entanglement is shared between two qubits in a multiparticle state is very crucial for tasks like teleportation and superdense coding. It has been seen that the asymmetric $|W\rangle$ state can teleport with a higher fidelity, whereas the $|W\rangle$ state fails.

Thus the modified W state can be a key source for quantum protocols as different tasks can be performed in accordance with the requirement. This state has been subjected to extensive study in the past few years. Proposals using cavity QED experiments for generating these states have been given[75]. Considering the importance of these states, an experimental proposal of generating these states using exchange interaction between the qubits in quantum dot systems, is given in the next section. This is then further generalized to N qubits.

Let us consider a 3-qubit state, which is an eigen state of the total $\hat{S^z} = \sum_{i=1}^{3} S_i^z$ operator given by,

$$|W_3\rangle = \alpha_1|100\rangle + \alpha_2|010\rangle + \alpha_3|001\rangle, \tag{62}$$

where, $|\alpha_1|^2 + |\alpha_2|^2 + |\alpha_3|^2 = 1$. If one of the qubits, say the last one is given to Bob, and the other two are in Alice's possession, then, Alice can perfectly teleport a one qubit state $|\psi\rangle = a|0\rangle + b|1\rangle$ to Bob when the coefficients satisfy the following relation,

$$|\alpha_3|^2 = |\alpha_1|^2 + |\alpha_2|^2. \tag{63}$$

A simple state which satisfies the above condition, is the modified $|W\rangle$ state given in Eq. 58. With a more general parametrization, one can show that, $\alpha_1 = \frac{1}{\sqrt{2}}$, $\alpha_2 = \frac{1}{\sqrt{2}}\sin\phi e^{\iota\chi_1}$ and $\alpha_3 = \frac{1}{\sqrt{2}}\cos\phi e^{\iota\chi_1}$, where, $0 \le \phi \le 2\pi$ and similarly, $0 \le \chi_1, \chi_2 \le 2\pi$. On the contrary, if Bob is given the first qubit in the state $|W_3\rangle$, then for perfect teleportation,

$$|\alpha_1|^2 = |\alpha_2|^2 + |\alpha_3|^2. \tag{64}$$

Conditions given in Eq. 63 and Eq. 64 lead to completely different states. One can see that the imbalance in the weights of the basis states $|1\rangle$ and $|0\rangle$ for each qubit is responsible for such conditions. To overcome these imbalances, one can construct a W-like state,

$$|\tilde{W}_3\rangle = \frac{1}{2}\Big[|100\rangle + |010\rangle + |001\rangle + |111\rangle\Big], \tag{65}$$

where the basis states of all qubits are on equal footing. The problem with the above state is that it does not conserve the total $\hat{S}_z$, and hence becomes difficult to generate using simple interactions.

7. Physical realization of magnon state

As mentioned in the last section, N-qubit GHZ states and W states are very useful for teleportation. W states can be generated from a modified N-qubit interactions which conserve the $\hat{z}$ component of the total spin of qubits. These states are nothing but one magnon excitations of a ferromagnetic ground state. Here we shall use Heisenberg exchange interaction between qubits to generate N-magnon entangled channels for teleporting an unknown quantum state perfectly. Multi-electron quantum dot systems can be a possible realization for the schemes that we propose in generating the desired entangled states[57]. Spins of electrons in quantum dots have been proposed to be good candidates for quantum computation[58]. With the state-of-the-art technology in manufacturing and manipulating semiconductor nanostructures, quantum dots show the promise for scalable quantum computing[59,60]. With a high level of control over the number of electrons[61], and the applied external fields, desirable initial states can be achieved. The interaction between any two electronic spins can be controlled by the applied gate voltages[59,63]. The exchange interaction induced quantum gates, for example the $SWAP$ and $CNOT$ gates, have been implemented at picosecond time scales[58]. The nuclear spins on the $2D$ lattice give the dominant contribution to the decoherence of the electronic spin[60]. The time scales for this decay has been experimentally found to be of the order of a few nanoseconds[62,63]. The effect of the spin environment comes into the picture, either in repetitive usage of the dot, or, when there are large number of operations to be performed with these systems. The fidelity calculations show that one can perform 10^2–10^3 gate operations before the real loss of spin polarization of the electrons.

As has been done earlier, the three qubit exchange interaction can be described by the following Hamiltonian,

$$\mathcal{H} = J\vec{S}_A.\vec{S}_B + J\vec{S}_B.\vec{S}_C + J\Delta\vec{S}_A.\vec{S}_C, \tag{66}$$

where, J is the strength of the interaction. The exchange interaction is typically of the order of 0.01eV in strongly interacting systems. The parameter Δ determines the closeness of the 3-qubit chain. If $\Delta = 1$, this is a perfectly closed chain and for $\Delta = 0$, it is an open chain. We shall show how different kinds of $|W_3\rangle$ states can be generated by varying this parameter Δ.

The above Hamiltonian can be diagonalized in a straightforward manner, and the time evolution of various 3-qubit states can be found. We shall start with an initial 3-qubit state, $|\psi(0)\rangle = |100\rangle$. Since the Hamiltonian given in Eq. 66 conserves the $\hat{z}$ component of the total spin, i.e., $[\mathcal{H}, \sum_k S_k^z] = 0$, where, $k = A, B, C$, the state at a later time will be

$$|\psi(t)\rangle = \alpha_1(t)|100\rangle + \alpha_2(t)|010\rangle + \alpha_3(t)|001\rangle, \tag{67}$$

where the time dependent coefficients are given by

$$\begin{aligned}
\alpha_1(t) &= \frac{1}{6}\Big[2\mathrm{e}^{-itE_1} + 3\mathrm{e}^{-itE_2} + \mathrm{e}^{-itE_3}\Big], \\
\alpha_2(t) &= \frac{1}{3}\Big[\mathrm{e}^{-itE_1} - \mathrm{e}^{-itE_3}\Big], \\
\alpha_3(t) &= \frac{1}{6}\Big[2\mathrm{e}^{-itE_1} - \mathrm{e}^{-itE_2} + \mathrm{e}^{-itE_3}\Big].
\end{aligned} \tag{68}$$

The eigenvalues $E_1 = J(2+\Delta)/4, E_2 = 3J/4, E_3 = J(\Delta-4)/4$. The condition for perfect teleportation (when the first qubit is given to Bob), given in Eq. 64, for the above state gives,

$$3\cos\left(Jt\frac{1+2\Delta}{2}\right) + \cos\frac{3Jt}{2} + \frac{3}{2}\cos((1-\Delta)Jt) - 1 = 0. \tag{69}$$

One can now extract the times for which the above equation is satisfied. If the interaction between the qubits is switched off at those times, the three qubit state obtained will be the one which can be used as a perfect teleportation channel.

For perfectly closed chains corresponding to $\Delta = 1$, Eq. 69 yields the solution, which has a periodicity of $4\pi/3$, given by

$$Jt = \frac{2}{3}\cos^{-1}\Big(-\frac{1}{8}\Big). \tag{70}$$

In addition to this one also finds that $|\alpha_1(t)^2| = \frac{1}{2}$ and $|\alpha_2(t)|^2 = |\alpha_3(t)|^2 = \frac{1}{4}$, at the above given time. The three qubit state at time "t", is given by,

$$\begin{aligned}
|\psi(t=\tau)\rangle &= \frac{1}{2}\Big[\sqrt{2}\mathrm{e}^{\iota\phi_1}|100\rangle \\
&\quad + \mathrm{e}^{\iota\phi_2}|010\rangle + \mathrm{e}^{\iota\phi_2}|001\rangle\Big],
\end{aligned} \tag{71}$$

where $\tau = \frac{2}{3}[2n\pi + \cos^{-1}(-\frac{1}{8})]$, and $\phi_1 = \tan^{-1}(-\sqrt{2})$ and $\phi_2 = \tan^{-1}(\frac{\sqrt{2}}{3})$. Since we are

interested to give the first qubit to Bob, we have started with the initial state $|100\rangle$. Instead, if the last qubit have to be given to Bob, we would have started with the initial state $|001\rangle$.

The above analysis can be extended to the case of an N qubit channel with one magnon excitation and single qubit teleportation can be achieved using this. This can also be generalized to find out the n magnon states which can then be used for perfectly teleporting a one qubit state[57]. The exchange interaction among spin-1/2 particles can be used to generate a class of multi qubit entangled channels, which can then be used for teleportation. It was shown in Ref. 57 that for times $t = \frac{1}{J}\cos^{-1}(-1/8)$, one obtains the N qubit entangled state which can be used for teleportation. For a typical quantum dot system this time scale can be of the order of picoseconds. For smaller number of qubits these states can be generated periodically, whereas for large N there exists a unique time where one can obtain such entangled states.

8. Conclusion

In the last decade or so, there has been tremendous development in the area of quantum information processing, especially in accomplishing certain tasks like quantum teleportation, dense coding etc., both in the theoretical as well as experimental domains. To carry out these tasks, the key ingredient in a quantum mechanical system is entanglement. Spin chains have proven to be a useful channel to execute some of these quantum protocols and thus have been dealt with in some detail here. In absence of naturally available spin chains, an array of quantum dots can be used where one has more flexibility in entangling spins in adjacent dots by switching the interactions on and off at will. Theoretical proposals to test entanglement properties of low dimensional quantum systems have been given and compared with observed experimental data in organometallic compounds. Decoherence poses enormous hindrances in carrying out these quantum tasks and a lot of work is being done to beat the effects of decoherence. We give a specific example, where, the environment can lead to counterintuitive effect like preferential choice of basis for carrying out quantum tasks. Entanglement in many body systems, along with techniques for avoiding decoherence, will occupy researchers for years to come.

Received 14 April 2009.

References

1. E. Schroedinger, Proc. Camb. Phil. Soc. 31, 555 (1935).
2. A. Einstein, B. Podolsky and N. Rosen, Phys. Rev. 47, 777 (1935).
3. J.S. Bell, Speakable and Unspeakable in Quantum Mechanics, Cambridge University Press (1988).
4. M. A. Nielsen and I. L. Chuang, Quantum Computation and Quantum Information, Cambridge University Press (2000).
5. For a recent review, see L Amico, R Fazio, A Osterloh, and V Vedral, Rev. Mod. Phys. 80, 517 (2008).
6. C. Bennett *et al.*, Phys. Rev. Lett. 70, 1895 (1993).
7. P. Agrawal and A. Pati, Phys. Rev. A 74, 062320 (2006).
8. Sandrine Heutz, Chiranjib Mitra, Wei Wu, Andrew J. Fisher, Andrew Kerridge, Marshall Stoneham, Tony H. Harker, Julie Gardener, Hsiang-Han Tseng, Tim S. Jones, Christoph Renner, and Gabriel Aeppli, Adv. Mater., 19, 3618 (2007).
9. J. van den Brink and A. F. Morpurgo, Nature 450, 177 (2007).
10. S. A. Wolf, D. D. Awschalom, R. A. Buhrman, J. M. Daughton, S. von Molnr, M. L. Roukes, A. Y. Chtchelkanova, D. M. Treger, Science 294, 1488 (2001).
11. N. B. McKeown, in Phthalocyanine Materials: Synthesis, Structure and Function, Cambridge University Press, Cambridge (1998).
12. J. G. Xue, B. P. Rand, S. Ushida, S. R. Forrest, Adv. Mater. 17, 66 (2005).
13. R. F. Service, Science 310, 1762 (2005).
14. A. B. P. Lever, J. Chem. Soc. 1821 (1965).
15. K. Awaga, Y. Maruyama, Phys. Rev. B 44, 2589 (1991).
16. Y. Taguchi, T. Miyake, S. Margadonna, K. Kato, K. Prassides, Y. Iwasa, J. Am. Chem. Soc. 128, 3313 (2006).
17. H. Yamada, T. Shimada, A. Koma, J. Chem. Phys. 108, 10256 (1998).
18. Wei Wu, A. Kerridge, A. H. Harker, and A. J. Fisher, Phys. Rev. B 77, 184403 (2008).
19. J. C. Bonner, M. E. Fisher, Phys. Rev. 135, A640 (1964).
20. L. Noodleman, J. Chem. Phys. 74, 5737 (1980)
21. M. J. Frisch et al., Gaussian 98 Revision A11.4, Gaussian Inc., Pittsburgh, PA (2002).
22. C. Lee, W. Yang, R. G. Parr, Phys. Rev. B 37, 785 (1988).
23. A. D. Becke, J. Chem. Phys. 98, 5648 (1993).
24. E. Ruiz, P. Alemany, S. Alvarez, J. Cano, J. Am. Chem. Soc. 119, 1297 (1997).
25. P. W. Anderson, Phys. Rev. 115, 2 (1959).
26. (a) M. A. Ruderman, C. Kittel, Phys. Rev. 96, 99 (1954); (b) T. Kasuya, Prog. Theor. Phys. 16, 45 (1956), (c) K. Yosida, Phys. Rev. 106, 893 (1958).
27. C. G. Barraclough, A. K. Gregson, S. Mitra, J. Chem. Phys. 60, 962 (1974).
28. H. Miyoshi, J. Phys. Soc. Jpn. 37, 50 (1974).
29. M. Wieśniak, V. Vedral and C. Brukner, New Journal of Physics 7, 258 (2005).
30. C. Brukner, V. Vedral and A. Zeilinger, Phys. Rev. A 73, 012110 (2006).
31. V. Vedral, Nature 453, 1004 (2008).
32. C. Brukner and V. Vedral, e-print arXiv:quant-ph/0406040.
33. Asher Peres, Quantum Theory: Concepts and Methods, Kluwer Academic Press (1993).
34. Arnesen, M., S. Bose, and V. Vedral, Phys. Rev. Lett. 87, 017901 (2001).
35. W.K. Wootters, Phys. Rev. Lett. 80, 2245 (1998).
36. K.M. O'Connor and W.K. Wootters, Phys. Rev. A 63, 052302 (2001).
37. G. Xu et al., Phys. Rev. Lett. 84, 4465 (2000).
38. Berger *et al.*, Phys. Rev. 132, 1057 (1963).
39. D. D. Bhaktavatsala Rao, P. K. Panigrahi and Chiranjib Mitra, Phys. Rev. A 78, 022336 (2008).
40. *Theory of Open Quantum Systems* by H. P. Breuer and F. Petruccione, (Oxford University Press, London 2002)
41. N V Prokof'ev and P C E Stamp, Rep. Prog. Phys. 63, 669 (2000).
42. D. D. Bhaktavatsala Rao, V. Ravishankar, and V. Subrahmanyam, Phys. Rev. A 74, 22301 (2006).

43. H. P. Breuer, D. Burgarth, and F. Petruccione, Phys. Rev. B 70, 045323 (2004).
44. C. Bennett *et al.*, Phys. Rev. Lett. 70, 1895 (1993).
45. S. Oh, S. Lee and H. W. Lee, Phys. Rev. A 66, 022316 (2002).
46. P. Badziag, M. Horodecki, P. Horodecki and R. Horodecki Phys. Rev. A 62, 012311 (2000).
47. S. Muralidharan and P. K. Panigrahi, Phys. Rev. A 77, 032321 (2008).
48. K. W. Choo and L. C. Kwek, Phys. Rev. B 75, 205321 (2007).
49. O. Sauret, D. Feinberg and T. Martin, Eur. Phys. J. B 32, 545 (2003).
50. F. Benatti, R. F. Floreanini, and M. Piani Phys. Rev. Lett 91, 70402 (2003).
51. A. S. Bracker *et al.*, Phys. Rev. Lett. 94, 047402 (2005).
60. W. A. Coish and D. Loss, Phys. Rev. B 72, 125337 (2005).
53. P. Walther, K. J. Resch, T. Rudolph, E. Schenck, H. Weinfurter, V. Vedral, M. Aspelmeyer and A. Zeilinger *et al*, Nature 434, 169 (2005).
54. I. D. K. Brown, S . Stepney, A . Sudbery, and S . L. Braunstein, J. Phys. A: Math. Gen. 38, 1119 (2005).
55. M. Blasone, F. Dell'Anno, S. De Siena, and F. Illuminati, Phys. Rev. A 77, 062304 (2008).
56. S. Muralidharan and P. K. Panigrahi, Phys. Rev. A 77, 032231 (2008).
57. D. D. Bhaktavatsala Rao, Sayantan Ghosh, and Prasanta K. Panigrahi, Rev. A 78, 042328 (2008).
58. D. Loss and D. P. DiVincenzo Phys. Rev. A 57, 120 (1998).
59. J. R. Petta, A. C. Johnson, J. M. Taylor, E. A. Laird, A. Yacoby, M. D. Lukin, C. M. Marcus, M. P. Hanson, and A. C. Gossard, Science 309, 2180 (2005).
60. J. Schliemann, A. Khaetskii, and D. Loss, J. Phys.: Condens. Matter 15, 1809 (2003).
61. R. C. Ashoori, Nature 379, 413 (1996).
62. T. Fujisawa, D. G. Austing, Y. Tokura, Y. Hirayama, and S. Tarucha, Phys. Rev. Lett. 88, 236802 (2002).
63. E. A. Laird, J. R. Petta, A. C. Johnson, C. M. Marcus, A. Yacoby, M. P. Hanson, and A. C. Gossard, Phys. Rev. Lett. 97, 056801 (2006).
64. R. Hanson, L. P. Kouwenhoven, J. R. Petta, S. Tarucha, and L. M. Vandersypen, Rev. Mod. Phys. 79, 1217 (2007).
65. A. Vidan and R. M. Westervelt, Appl. Phys. Lett. 85, 3602 (2004).
66. C. H. Bennett, G. Brassard, C. Crepeau, R. Jozsa, A. Peres, and W. K. Wootters, Phys. Rev. Lett. 70, 1895 (1993).
67. D. Bouwmeester, J. W. Pan, K. Mattle, M. Eibl, H. Weinfurter, and A. Zeilinger, Nature (London) 390, 575 (1997).
68. M. D. Barrett, J. Chiaverini, T. Schaetz, J. Britton, W. M. Itano, J. D. Jost, E. Knill, C. Langer, D. Leibfried, R. Ozeri, and D. J. Wineland, Nature (London) 429, 737 (2004).
69. M. A. Nielsen, E. Knill and R. Laflamme, Nature 396, 52 (1998).
70. F. Benatti, R. F. Floreanini, and M. Piani Phys. Rev. Lett 91, 70402 (2003).
71. A. Karlsson and M. Bourennane, Phys. Rev. A 58, 4394 (1998).
72. Asher Peres, Phys. Rev. Lett. 77, 1413 (1996); M. Horodecki, P. Horodecki, R. Horodecki, Physics Letters A 223, 1 (1996).
73. L. Li and D. Qiu, J. Phys. A 40, 10871 (2007).
74. M. Hillery, V. Buzek, and A. Berthiaume, Phys. Rev. A 59, 1829 (1999).
75. Dong Li, Xiu Xiao-Ming, Gao Ya-Jun and Chi Feng, Communications in Theoretical Physics 49, 1495 (2008).
76. He Juan, Ye Liu, Ma Chi, Liu Qi and Ni Zhi-Xiang, Communications in Theoretical Physics 49, 617 (2008).
77. D. D. Bhaktavatsala Rao, V. Ravishankar, and V. Subrahmanyam, Phys. Rev. A 74, 22301 (2006).

Dr. P. K. Panigrahi's primary interest are in the area of Cold Atoms, Quantum Computation and Field Theory. In cold atoms, unusual pairing mechanisms, the structure of unitary fermi gas & solitonic excitations in Bose Einstein Condensates are under current investigation. Implementation of various communication protocols & their security are being pursued in the area of Quantum Computation. Watching birds and plants are amongst his other interests.

Dr. Chiranjib Mitra's interests are in the area of Quantum Magnetism, Spintronics, Quantum Computation and Nanotechnology. In quantum computation and quantum magnetism, his primary interests lie in extracting entanglement from spin chains and other low dimensional systems. In addition to that he is also keen on spin dynamics of isolated spin qubits and coupled qubits. He intends to make a workable quantum computer using magneto-optical techniques. Trekking, long distance running, working out in the gym and nature photography are amongst his interests.